Biomedicine and Chemical Sciences 1(3) (2022) 138-146

20-BCS-830-187

Contents lists available at:
https://journals.irapa.org/index.php/BCS/issue/view/12

Biomedicine and Chemical Sciences

Journal homepage: https://journals.irapa.org/index.php/BCS

New Homo and Heterobinuclear Macrocyclic Complexes Bearing Isatine: Structural Characterization, Thermal Study and DFT Calculations

Anaam Rasheed[a], Senan Albayati[b], Sarab Alazawi[c], Enas Zuhair[d], Mudeer Merza[e], Khalil Abid[f*]

[a,b,c,d,e,f] *Department of Chemistry, College of Science, Mustanseriyah University, Baghdad - Iraq*

ARTICLE INFO

Article history:
Received on: February 28, 2022
Revised on: March 28, 2022
Accepted on: March 28, 2022
Published on: July 01, 2022

Keywords:
Bimetal Complexes
Diaminopyridine
Schiff Base
Supermolecule Ligands

ABSTRACT

A new metal-free macrocyclic Schiff base ligand bearing two metal cavities incorporated with two sets of N_3O_2 donor atoms derived from 2, 6-diaminopyridine and isatine was synthesized. The new ligand was used to prepare homo and hetero binuclear macrocyclic Schiff base complexes with Ni (II), Cu (II), ZrO (II) and Ba (II) metal ions. The ligand and metal complexes were characterized using Fourier transform infrared (FT-IR), UV–vis, mass spectroscopy, elemental analysis (CHN), thermo gravimetric analysis (TGA), magnetic susceptibility, and molar conductivity measurements. The DFT calculations using the B3LYP functional method have been applied to obtain the geometry and electronic properties of the ligand and its metal complexes to support the experimental data. To describe the reactivity of the title molecules, the HOMO and LUMO levels and Mulliken atomic charges were determined.

1. Introduction

Coordination chemistry of macrocyclic ligands have demonstrated an extensive intrigue over the most recent two decades (Archibald, 2009; Chu, et al., 2008). The utilization of macrocyclic ligands as models for protein-metal binding sites in biological systems, such as the synthetic ionophores, models for the magnetic exchange phenomena, therapeutic reagents in chelate therapy for treatment of metal intoxication and the cyclic antimicrobials that hold their anti-toxin activities to specific metal complexation raises the importance of new macrocyclic ligand designing (Kilpin, et al., 2007; Tušek-Božić, et al., 2007). Macrocyclic systems got extra significance over the acyclic ligand systems as the macro systems are thermodynamically stabilized and kinetically delayed toward metal dissociation and substitution by the so-called 'macrocyclic effect'. The incredible significance of macrocyclic systems in chemistry properly because of their particular chelation towards certain metal particles relying upon the number, size of the cavity, type, number and position of their donor atoms. The ionic radii of the metal centers and the coordination property of the counter ions (Ceramella, et al., 2022) gives them the exceptional significance in the field of bioinorganic chemistry (Gull, et al., 2017; Ikotun, et al., 2019) and the potential therapeutic, analytical and industrial applications (Chandra & Kumar, 2004; Chandra, et al., 2006). Schiff base metal complexes show a broad range of biological activity that is usually increased by complexation with the metal ion. It have striking properties such as antibacterial, antifungal, antiviral, antiinflammatory, anti-tumor and cytotoxic activities, plant development controller, enzymatic activity and applications in pharmaceutical fields (Bitu, et al., 2019).

Buildup of diamines and dialdehydes to form Schiff base macrocycles has been utilized by numerous researches to frame both small and enormous stable macrocycles, usually templated with transition metals (Ma, et al., 2006; Beckmann & Brooker, 2003). Nontemplate macrocyclic Schiff base synthesis process requires the use of rigid starting carbonyl groups and high dilution conditions. This process is very efficient and the metal free product can be obtained in good yield. Synthetic macrocyclic complexes mimic some naturally occurring macrocycles because of

*Corresponding author: Khalil Abid, Department of Chemistry, College of Science, Mustanseriyah University, Baghdad - Iraq
E-mail: abidk56@yahoo.com

How to cite:
Rasheed, A., Albayati, S., Alazawi, S., Zuhair, E., Merza, M., & Abid, K. (2022). New Homo and Heterobinuclear Macrocyclic Complexes Bearing Isatine: Structural Characterization, Thermal Study and DFT Calculations. Biomedicine and Chemical Sciences, 1(3), 138-146.
DOI: https://doi.org/10.48112/bcs.v1i3.187

their resemblance with many natural macrocycles, such as metalloproteins and metalloenzymes. Some macrocyclic complexes have gotten exceptional consideration as a result of their have received special attention because of their mixed soft–hard donor character and versatile coordination behaviour and because of their pharmacological properties, i.e., lethality against bacterial and contagious development. One significant point of intrigue is to create homo and hetero-multimetallic complexes since they show distinct reactivity design when compared with comparing monometallic complexes. The magnetic interactions and coupling between the metal ions present in such complexes play key role in both natural and synthetic catalysts. Several attempts to prepare heterobinuclear complexes from the mononuclear ones were unsuccesfsull, yielding the starting materials or homobinuclear complexes (Mohapatra, et al., 2012; Borisova, et al., 2004).

Isatin considered as one of the raw materials for the drug synthesis due to its cis α-dicarbonyl moiety, it is one of the essential substrates to synthesize metal complexes. Deprotonated or alone, it might be located in the mammalian tissues, stemming from the interests in pharmacological and biological characteristics of isatin derivatives (Alkam, et al., 2021). The present work is focused on synthesis and structural characterization of new macrocyclic Schiff base ligand bearing isatine moiety and its homo – and heterobinuclear complexes with Ni (II), Cu (II), ZrO (II) and Ba (II) metal particles. Additionally, the results of the calculations of DFT as well as geometry optimization of the synthesized molecules were reported.

2. Materials and Methods

All chemicals were analytical grade and used without any modification. Electronic spectra were obtained by use of a Varian UV–Vis spectrophotometer, molar conductivity measurements by use of a WTWF56 apparatus with absolute ethanol as solvent, and FTIR spectra by use of a Shimadzu spectrophotometer, mass spectra were recorded by use of Schimadzu mass spectroscopy, Magnetic susceptibility measurements were carried out using of Curie balance in the Chemistry Department, College of Science, Mustansiriya University. Flame atomic absorption, Elemental analysis (C.H.N.) performed with an elemental analyzer (EA) and thermal stability (weight changes) of the samples were recorded by Mettler Toledo in the temperature up to 600 °C in the Ibn Alhatham College of Pure Science, University of Baghdad, Iraq. The DFT calculations using B3LYP functional method has been applied to obtain the geometry and electronic properties of the ligand and its metal complexes.

2.1. Preparation of Preliminarily Compound

This compound was prepared according to the procedure mentioned in literature (Dileepan, et al., 2018). 2 g, 0.013 mol of isatin dissolved in 30 mL of ethanol and 0.54 g, 0.013 mol of NaOH dissolved in 20 mL of distilled water and 0.52 g, 0.006 mol of dibromoethane were mixed in a 250 mL round bottom flask, and this mixture was heated at 70 °C in water bath for 16 hr. After completion of the reaction as monitored by TLC, the reaction mixture was cooled and washed with hot water. The solid residue was extracted twice with dichloromethane (50 and 20 mL respectively) and the solution was brought to dryness, and then washed with methanol. The obtained solid was dried under vacuum to give a pale yellow colored product.

2.2. Synthesis of Metal Free Macrocyclic Schiff Base Ligand

0.002 mol of compound 1 dissolved in ethanol (20 mL) mixed with 0.002 mol of 2,6-diaminopyridine dissolved in absolute ethanol (30 mL) and few drops of glacial acetic acid were added as catalyst. The mixture was refluxed for 8 hr, cooled and filtered. The solid product was recrystallized from ethanol to afford a bright orange crystals in 84 % yield (Scheme 1).

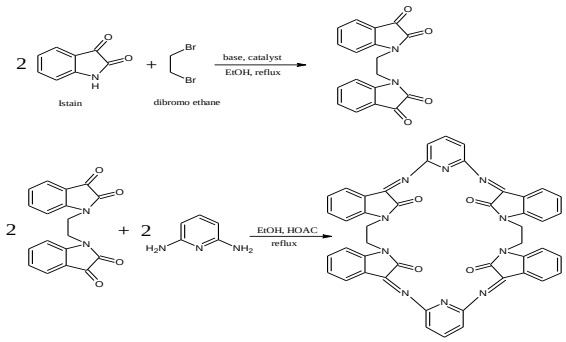

Scheme 1 Synthesis of Macrocyclic Schiff base ligand(L)

2.3. Synthesis of Homobinuclear Metal Complexes

To a stirred solution of 0.001 mol of the ligand in ethanol (40 mL) and 0.002 mol of metal salt ($NiCl_2.6H_2O$, $CuCl_2.2H_2O$, $ZrOCl_2.6H_2O$ and $BaCl_2.2H_2O$) in ethanol (30 mL) were mixed under reflux for 3 hr. The resultant precipitate were cooled, filtered off and washed with cold water and ethanol then dried in oven for 3 hr at 70 ^oC.

2.4. Synthesis of Heterobinuclear Metal Complexes

The mononuclear metal complexes were obtained first by the reaction of 0.001 mol of $NiCl_2.6H_2O$ in ethanol (20 mL) and slightly access (0.001 mol) of the macrocyclic ligand in ethanol (20 mL) at reflux for 3 hr to afford a brown precipitate which filtered off and dried. 0.001 mol of this complex in warm ethanol (20 mL) was mixed with 0.001 mol of $CuCl_2.2H_2O$ in warm ethanol (20 ml). A green precipitate of heterobinuclear complex ($NiCuL.Cl_4$) was formed instantaneously, stirring to complete the reaction for additional 1 hr, filtered off, washed with cold ethanol and dried in oven for 3 hr at 70 ^oC, Table 1.

2.5. Computational Details

Gaussian 09 (with Gaus view 5.08) suite of programs has been conveyed for completing all calculations and assessments of the study. Complete optimization of all complex's geometries at B3LYP at the level LanL2DZ was performed. Accordingly, it is sent regularly alongside the techniques for density functional for completing the investigation of transition metals containing frameworks.

Table 1
Some physical and chemical properties of the ligand and metal complexes

%Elemental Analysis Found(Calc.)				Conduct.	M.P.	M.Wt	Colour	Compound
				ohm⁻¹ cm² / mol	^{0}C	*g / mol*		
M%	N	H	C					
----	17.81 (17.78)	3.81 (3.79)	70.22 (70.2)	----	166-168	786	Deep Orange	L $C_{46}H_{30}N_{10}O_4$
6.82 (6.41)	15.39 (15.28)	3.31 (3.27)	60.4 (60.28)	87	220	915.7	Light Brown	$[NiL]Cl_2$
11.42 (11.19)	13.39 (13.37)	2.86 (2.85)	52.8 (52.77)	156	252d*	1045	Green	$[Ni_2L(H_2O)_2]Cl_4$
12.33 (12.02)	13.27 (13.19)	2.84 (2.83)	52.32 -51.99	153	260	1055	Deep Brown	$[Cu_2L]Cl_4$
23.29 (23.01)	11.64 (11.59)	2.49 (2.42)	45.92 (45.88)	158	300d*	1202	Light Green	$[Ba_2L]\ Cl_4$
15.43 (14.99)	12.25 (12.20)	2.62 (2.57)	48.33 (48.28)	155	274d*	1142	Brown	$[(ZrO)_2\ L\ ]Cl_4$
12.15 -11.63	13.41 (13.33)	2.91 (2.85)	52.67 (52.57)	151	240d*	1050	Olive Green	$[NiCu(\ L)]Cl_4$

3. Results and Discussion

3.1. FT – IR spectra

The (FT-IR) spectra were recorded in the region 4000–400 cm^{-1} by using KBr disc. The IR spectra of preliminarily compound showed a characteristic bands at 3065, 3271 and 1731 cm^{-1} attributed to aromatic, aliphatic (C– H) and (C = O) groups respectively (Silverstein & Bassler, 1962; Racles, et al., 2013). The formation of macrocyclic Schiff base ligand was confirmed by the presence of the azomethine band at 1656 cm^{-1} while the position of the carbonyl group was shifted to 1722 cm^{-1}. The spectra of metal complexes showed clear red shift in the absorptions of these bonds (Venkatesh & Geetha, 2015), these indicates the coordination of the Ni (II), Cu (II), ZrO (II) and Ba (II) metal ions with these active sites. The mononuclear complexes showed two absorption bands for each of υ(C=O) and υ(C=N) bonds which probably assigned to one corrdinated and one uncoordinated cavity. The presence of coordinated water molecule for Ni (II) complex was indicated by the appearance of a broad band around 3450 cm^{-1} and two weak bands at 765, 712 cm^{-1} respectively due to (-OH) rocking and wagging mode of vibrations. The frequency of Zr = O band was located at 1418 cm^{-1}, while two new bands appeared in the complexes around 550 and 450 cm^{-1}; these were attributed to the coordinated M–N and M–O bonds respectively (Nakamoto, 2009), see Table S1 in supplementary data.

3.2. UV–Visible Spectra

The ligand and metal complexes were recorded in 200 – 800 nm using concentration of 0.001 M and absolute ethanol as a solvent. The high energy around 217 nm is probably related to π→π* transitions centered on the benzene moiety. Other absorption bands were observed around 260 and 322 nm probably assignment to n→π* transitions. The electronic spectra of metal complexes showed considerable red shift (15 – 30 nm) in the λmax values of n→π* absorption bands in comparison with the free ligands. These red shifts are presumably due to the nephelauxetic effect and are regarded as a measure of covalence of the bonding between the metal ion and the ligands, suggest weak covalent nature of the metal–ligand bonds (Nockemann, et al., 2006). The new low energy band appeared around 440 nm for the metal complexes probably pronounced as charge transfer transition character. Three bands were recorded for the Ni (II) complex at 632, 491 and the third band combined with the charge transfer bands around 410 – 450 nm, these band attributed to the transitions $^3A_2g \rightarrow {}^3T_2g$ (F), $^3A_2g \rightarrow {}^3T_1g$ (F), and $^3A_2g \rightarrow {}^3T_1g$ (P), respectively, suggesting octahedral geometry. The relatively weak intensity broad band at 478 nm for Cu (II) complex assigned to $^2B_{1g} \rightarrow {}^2A_{1g}$ transition with high magentic moment observed, bond angels and length obtained for coordinated Cu – O and Cu – N bonds., confirming the square planar geometry around Cu^{+2} metal ion (Gliemann, 1985). For ZrO (II) and Ba (II) complexes and their configuration according to DFT calculation were square pyramid and tetrahedral geometry respectively (Figure 4).

3.3. Mass Spectra

Mass spectra were recorded using a Direct Injection Probe.The mass spectra of the ligand(L) illustrated in Figure 1 showed a molecular ion peak at *m / e* = 786 *g / mole* which agree well with the empirical formula of the ligand, $C_{46}H_{30}N_{10}O_4$. The base peak with relative *I* = 100 % of the peak at *m / e*= 57 may be resulted from the extreme stability of the fragment [*m / e* = C_2H_3NO .

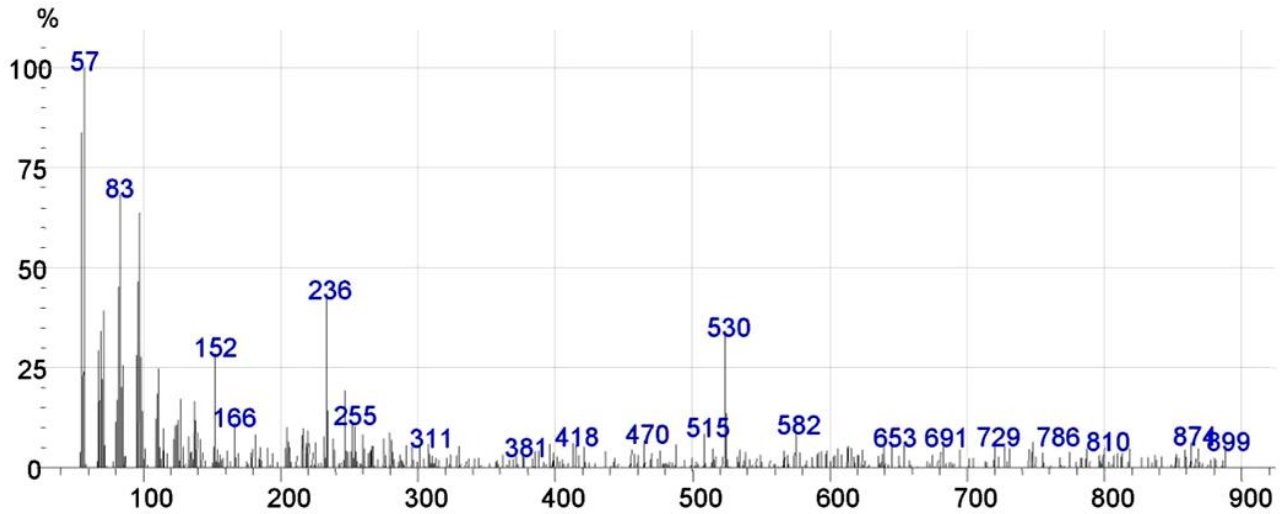

Fig. 1. Mass spectra of the ligand (L)

3.4. Magnetic Measurements

The magnetic susceptibility for the complexes was recorded in the solid state at 298 *K* using Faraday's method. All the prepared complexes of the Ni (II), ZrO (II) and Ba (II) ions showed diamagnetic properties since no electrons found in the valence shell of orbital for later two ions while it confirmed a low spin for Ni (II) complex. The homobinuclear Cu (II) and heterobinuclear Ni (II) Cu (II) complexes recorded a relatively high magnetic moment of 2.52 *B.M.* which support the squar planner – squar planar geometry for the first and octahedral – squar planar geometries for the second.

3.5. Molar Conductivity Measurements

The molar conductivity measurements for the complexes were carried out using a concentration of 10^{-3} M and absolute ethanol as a solvent and CON 510 bench conductivity meter (cell constant, *K* = 1.0) in order to assist us in the elucidation the formula and structures of the prepared homo- and heterobinuclear complexes. The data observed for molar conductance of bimetal complexes showed molar conductivity values in the range (124.3-146.5 $\Omega^{-1}\ cm^2 / mol$) which suggest a 1:4 electrolyte type, while the Ni (II) mononuclear complex showed conductivity of 64 $\Omega^{-1}\ cm^2 / mol$ agree with 1:2 electrolyte type. The collected results supports the four coordination number with equilibrium environments of squar planner geometry around Ni (II) and Cu (II), tetrahedral around Ba (II) and squar pyramide geometry around ZrO (II) ions.

3.6. Thermogravimetric Analysis of Metal Complexes

Thermogravimetric analyses of complexes were performed under air atmosphere at the heating rate 10°C / min up to 600 °C. The thermogram of Ni (II) complex recorded three stages of weight loose. The first one showed the initial weight loss in the temperature around 250 °C probably due to the loss of coordinated water molecule (Bottei & Quane, 1964). The anhydrous complexes remain stable up to 425 °C then the complex suffered a rapid and big weight loose due to the decomposition of macrocyclic ligand of the complex molecule followed by the final residue of NiO above 590 °C. The TGA curve of the other complexes do not show any weight loss below 290 °C and shows only two stages of mass loss at the temperature around 295 °C and 591 °C corresponding to the decomposition of the complex for the first and the formation of a thermally stable metal oxide for the second (Cifelli, et al., 2013). It is strong evidence, which represent that these complexes were devoid of lattice water as well as coordinated water in the coordination sphere (See Figures 2 and 3).

3.7. Structural Analysis

The optimized geometrical structures of the L and Ni (II), Cu (II) , ZrO (II) and Ba (II) complex molecules were shown in Figure 4. The selected bond lengths, bond angles, dipole moments and ev of HOMO, LUMO of these structures were calculated, Table S2 and S3 in supplementary data. The optimized structure obtained were agree with the suggested configurations of the metal complexes based on the experimental data. It gives a good evidence of octahedral geometry for Ni (II) stabilized by one water molecule with N_3O_2 atoms around metal atom, while the structures of Cu (II) , Ba (II) and ZrO (II) complexes were squar planner, tetrahedral and square pyramid respectively stabilized by N_2O_2 atoms.

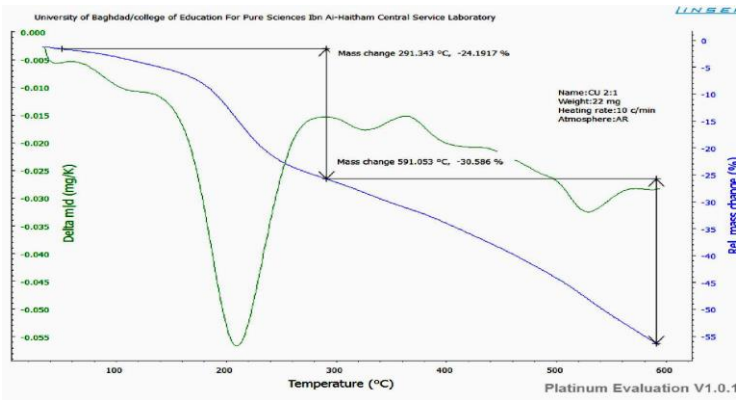

Fig. 2. TGA for [Cu_2 L] complex

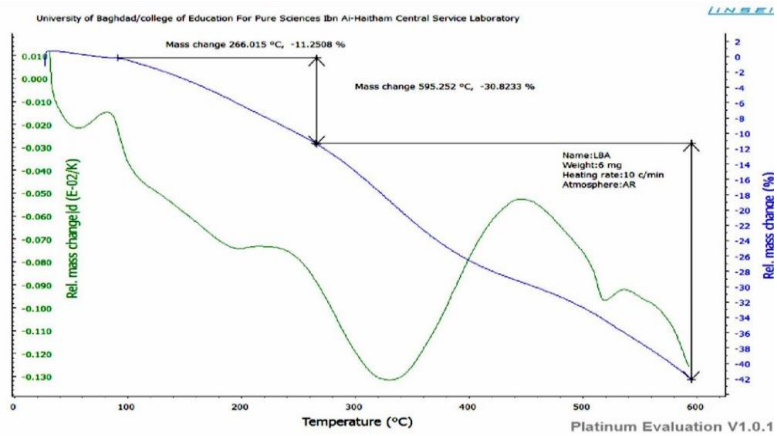

Fig. 3. TGA for [Ba_2 L] complex

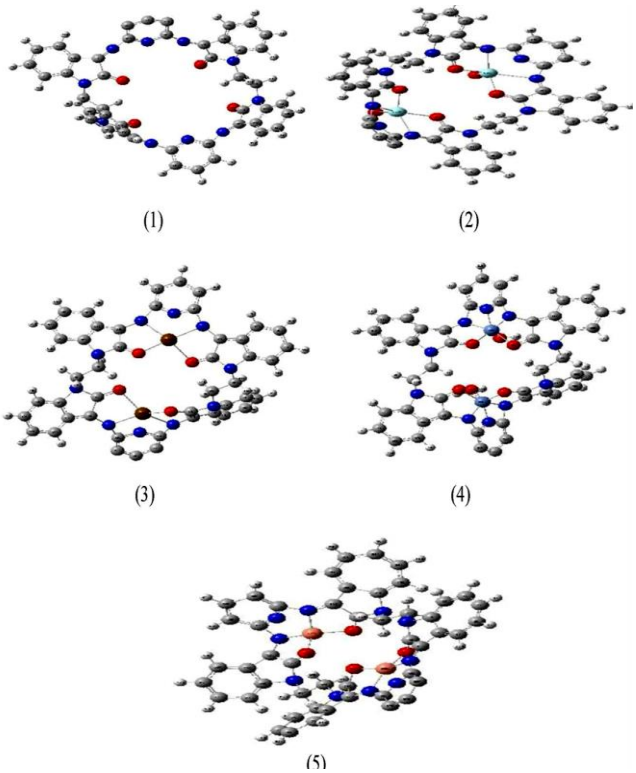

Fig. 4. The optimized structures of L, ZrO (II), Ba (II), Ni (II) and Cu (II) complexes respectively

3.8. HOMO-LUMO and MEP Analysis

In a molecule, the highest energy level (EHOMO) that is full of electrons and the lowest energy level (ELUMO) that is lack of electrons play an important role in electrical, optical, and molecular charge transfer (Arshad, et al., 2017; Sherzaman, et al., 2017). While HOMO orbitals tend to give electrons, which in turns it is suitable to form a coordination bonds with the metal ions, LUMO orbitals suffers luck of electrons and tends to receive them. These molecular orbitals (MOs) are important because their interaction with other molecules is through HOMO-LUMO priority orbitals. It shows the HOMO orbitals of the ligand were localized on the carbonyl group of the the isatin ring and azomethine group, while LUMO orbitals were localized on the benzene ring.

Molecular electrical potential surface (MEP) also known as electrostatic potentials map, or electrostatic potential energy map, was determined for the ligand. It illustrate the charge distributions of molecule three dimensionally. This map allows us to visualize variably charged regions of a molecule. Knowledge of the charge distributions can be used to determine how molecules interact with one another. They also allow us to visualize the size and shape of molecules. In organic chemistry, electrostatic potential maps are invaluable in predicting the behavior of complex molecules (see Figures S3, S4 and S5 in supplementary data).

4. Conclusion

This work is aimed at synthesizing new homo and heterobinuclear macrocyclic complexes through the two steps of substitution reaction to afford a macrocyclic Schiff base ligand bearing two cavities consisting of N_2O_2 donor atoms ready for complexing. The investigation of the collected experimental data of the ligand and the metal complexes combined with the DFT calculations showed the geometry of octahedral for Ni (II), squar planner for Cu (II), tetrahedral for Ba (II) and squar pyramide for ZrO (II) with a 2:1 molar ratio (M:L).

Acknowledgments

The authors would like to thank the Ibn Alhaitham College of Pure Science, University of Baghdad for spectral data and University of Mustansiriyah, College of Science for providing the financial support.

Competing Interests

The authors have declared that no competing interests exist.

References

Alkam, H. H., Atiyah, E. M., Majeed, N. M., & Alwan, W. M. (2021). Cupper (ii) and mercury (ii) complexes with schiff base ligands from benzidine with isatin and benzoine: synthesis, spectral characterization, thermal studies and biological activities. Systematic Reviews in Pharmacy, 12(1).

Archibald, S. J. (2009). Coordination chemistry of macrocyclic ligands. Annual Reports Section" A"(Inorganic Chemistry), 105, 297-322. **https://doi.org/10.1039/B818281G**

Arshad, M., Jadoon, M., Iqbal, Z., Fatima, M., Ali, M., Ayub, K., ... & Mahmood, T. (2017). Synthesis, molecular structure, quantum mechanical studies and urease inhibition assay of two new isatin derived sulfonylhydrazides. Journal of Molecular Structure, 1133, 80-89. **https://doi.org/10.1016/j.molstruc.2016.11.065**

Beckmann, U., & Brooker, S. (2003). Cobalt (II) complexes of pyridazine or triazole containing ligands: spin-state control. Coordination chemistry reviews, 245(1-2), 17-29. **https://doi.org/10.1016/S0010-8545(03)00030-4**

Bitu, M. N. A., Hossain, M. S., Zahid, A. A. S. M., Zakaria, C. M., & Kudrat-E-Zahan, M. (2019). Anti-pathogenic activity of cu (II) complexes incorporating Schiff bases: a short review. American Journal of Heterocyclic Chemistry, 5(1), 11-23. **https://doi.org/10.11648/j.ajhc.20190501.14**

Borisova, N. E., Reshetova, M. D., & Ustynyuk, Y. A. (2004). Binuclear and polynuclear transition metal complexes with macrocyclic ligands. 3. New polydentate macrocyclic ligands in reactions of 4-alkyl-2, 6-diformylphenols with 1, 2-diaminobenzenes. Russian Chemical Bulletin, 53(1), 181-188. **https://doi.org/ 10.1023/B:RUCB.0000024848.03470.25**

Bottei, R. S., & Quane, D. (1964). Preparation and thermal stability of some divalent metal chelate polymers of β-hydronaphthazarin. Journal of Inorganic and Nuclear Chemistry, 26(11), 1919-1925. **https://doi.org/10.1016/0022-1902(64)80017-8**

Ceramella, J., Iacopetta, D., Catalano, A., Cirillo, F., Lappano, R., & Sinicropi, M. S. (2022). A review on the antimicrobial activity of schiff bases: Data collection and recent studies. Antibiotics, 11(2), 191. **https://doi.org/10.3390/antibiotics11020191**

Chandra, S., & Kumar, R. (2004). Synthesis and spectral studies on mononuclear complexes of chromium (III) and manganese (II) with 12-membered tetradentate N2O2, N2S2 and N4 donor macrocyclic ligands. Transition Metal Chemistry, 29(3), 269-275. **https://doi.org/10.1023/B:TMCH.0000020359.84853.72**

Chandra, S., Gupta, R., Gupta, N., & Bawa, S. S. (2006). Biologically relevant macrocyclic complexes of copper spectral, magnetic, thermal and antibacterial approach. Transition Metal Chemistry, 31(2), 147-151. **https://doi.org/10.1007/s11243-005-6194-5**

Chu, Z., Huang, W., Wang, L., & Gou, S. (2008). Chiral 27-membered [3+ 3] Schiff-base macrocycles and their reactivity with first-row transition metal ions. Polyhedron, 27(3), 1079-1092. **https://doi.org/10.1016/j.poly.2007.12.003**

Cifelli, M., Domenici, V., & Veracini, C. A. (2013). Recent advancements in understanding thermotropic liquid crystal structure and dynamics by means of NMR spectroscopy. Current Opinion in Colloid & Interface Science, 18(3), 190-200. **https://doi.org/10.1016/j.cocis.2013.03.003**

Dileepan, A. B., Prakash, T. D., Kumar, A. G., Rajam, P. S., Dhayabaran, V. V., & Rajaram, R. (2018). Isatin based macrocyclic Schiff base ligands as novel candidates for antimicrobial and antioxidant drug design: In vitro DNA binding and biological studies. Journal of Photochemistry and Photobiology B: Biology, 183, 191-200. **https://doi.org/10.1016/j.jphotobiol.2018.04.029**

Gliemann, G. A. B. P. (1985). ABP Lever: Inorganic Electronic Spectroscopy, Vol. 33 aus: Studies in Physical and Theoretical Chemistry, Elsevier, Amsterdam, Oxford, New York, Tokio 1984. 863 Seiten, Preis: $113, 50. **https://doi.org/10.1002/bbpc.19850890122**

Gull, P., Babgi, B. A., & Hashmi, A. A. (2017). Synthesis of Ni (II), Cu (II) and Co (II) complexes with new macrocyclic Schiff-base ligand containing dihydrazide moiety: Spectroscopic, structural, antimicrobial and antioxidant properties. Microbial Pathogenesis, 110, 444-449. **https://doi.org/10.1016/j.micpath.2017.07.030**

Ikotun, A. A., Oladimeji, A. O., & Oluranti, O. O. (2019). Synthesis, Physicochemical and Antimicrobial Properties of Co (II) and Ni (II) metal complexes of the Schiff base of isatin and 4-methylaniline. Journal of Applied Sciences and Environmental Management, 23(11), 1957-1962. **https://dx.doi.org/10.4314/jasem.v23i11.8**

Kilpin, K. J., Henderson, W., & Nicholson, B. K. (2007). Synthesis, characterisation and biological activity of cycloaurated organogold (III) complexes with imidate ligands. Polyhedron, 26(1), 204-213. **https://doi.org/10.1016/j.poly.2006.08.009**

Ma, W., Tian, Y. P., Zhang, S. Y., Wu, J. Y., Fun, H. K., & Chantrapromma, S. (2006). Synthesis and characterization of 1, 8-bis (ferrocenylmethyl)-5, 5, 12, 12, 14-hexamethyl-1, 4, 8, 11-tetraazacyclotetradecane, a macrocyclic ligand and its complexes. Transition Metal Chemistry, 31(1), 97-102. **https://doi.org/10.1007/s11243-005-6336-9**

Mohapatra, R. K., Ghosh, S., Naik, P., Mishra, S. K., Mahapatra, A., & Dash, D. C. (2012). Synthesis and Characterization of Homo Binuclear Macrocyclic Complexes of UO 2 (VI), Th (IV), ZrO (IV) and VO (IV) with Schiff-Bases Derived from Ethylene diamine/Orthophenylene Diamine, Benzilmonohydrazone and Acetyl Acetone. Journal of the Korean Chemical Society, 56(1), 62-67. **https://doi.org/10.5012/jkcs.2012.56.1.062**

Nakamoto, K. (2009). Infrared and Raman spectra of inorganic and coordination compounds, part B: applications in coordination, organometallic, and bioinorganic chemistry. John Wiley & Sons. **https://doi.org/10.1002/0470027320.s4104**

Nockemann, P., Thijs, B., Postelmans, N., Van Hecke, K., Van Meervelt, L., & Binnemans, K. (2006). Anionic rare-earth thiocyanate complexes as building blocks for low-melting metal-containing ionic liquids. Journal of the American Chemical Society, 128(42), 13658-13659. **https://doi.org/10.1021/ja0640391**

Racles, C., Silion, M., Arvinte, A., Iacob, M., & Cazacu, M. (2013). Synthesis and characterization of poly (siloxane–azomethine) iron (III) coordination compounds. Designed Monomers and Polymers, 16(5), 425-435. **https://doi.org/10.1080/15685551.2012.747161**

Sherzaman, S., Ahmed, M. N., Khan, B. A., Mahmood, T., Ayub, K., & Tahir, M. N. (2017). Thiobiuret based Ni (II) and Co (III) complexes: synthesis, molecular structures and DFT studies. Journal of Molecular Structure, 1148, 388-396. **https://doi.org/10.1016/j.molstruc.2017.07.054**

Silverstein, R. M., & Bassler, G. C. (1962). Spectrometric identification of organic compounds. Journal of Chemical Education, 39(11), 546. **https://doi.org/10.1021/ed039p546**

Tušek-Božić, L., Marotta, E., & Traldi, P. (2007). Efficient solid-state microwave-promoted complexation of a mixed dioxa-diaza macrocycle with an alkali salt. Synthesis of a sodium ethyl 4-benzeneazophosphonate complex. Polyhedron, 26(8), 1663-1668. **https://doi.org/10.1016/j.poly.2006.12.012**

Venkatesh, R., & Geetha, K. (2015). Synthesis and Spectroscopic Investigation of Novel Nickel (II) Complexes from Pentadentate Schiff Base Ligand. SOJ Materials Science & Engineering, 3(2), 1-5. **http://dx.doi.org/10.15226/sojmse.2015.00121**

Supplementary Data for Manuscript

Table S1

Major Infra – red spectra of the ligand and complexes (cm^{-1})

Compound	$\nu_{(C=O)}$	$\nu_{(C=N)}$	$\nu_{(M-N)}$	$N_{(M-O)}$
$C_{46}H_{30}N_{10}O_4$	1722	1656	-	-
$[NiL]Cl_2$	1707, 1719	1641, 1653	565	472
$[Ni_2L(H_2O)_2]Cl_4$	1705	1643	563	468
$[Cu_2L]Cl_4$	1695	1638	570	480
$[Ba_2L]\ Cl_4$	1702	1635	543	443
$[(ZrO)_2\ L\ ]Cl_4$	1710	1650	525	418$_{(Zr=O)}$, 430

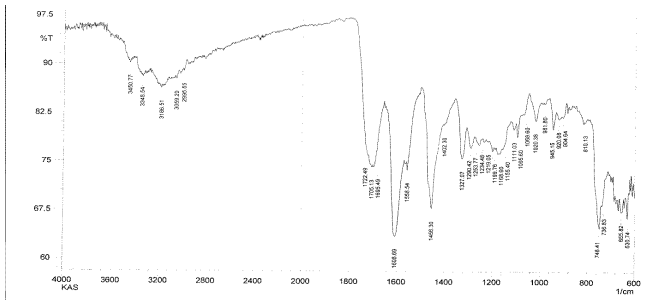

Fig. S1. Infrared spectra of the macrocyclic ligand

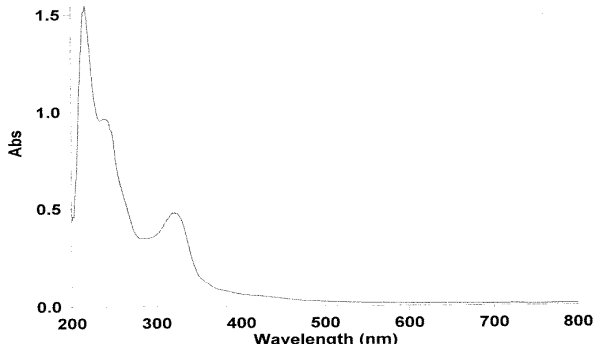

Fig. S2. UV - vis spectra of the macrocyclic ligand

Table S2

Selected calculated bond lengths [A] for ligand and metal complexes

Bond length	Ligand	Zr^{+2} Complex	Ni^{+2} Complex	Ba^{+2} Complex	Cu^{+2} Complex
N4-C1	1.2474648	1.3243446	1.3917231	1.3398398	1.321782
C5-N3	1.5021387	1.4701977	1.4669541	1.4975964	1.34046
N11-C9	1.3330117	1.3325369	1.4680986	1.4188147	1.070128
O12-C9	1.2508565	1.3240249	1.3278668	1.3392561	1.069501
N13-C10	1.1999732	1.3549573	1.3986174	1.3335973	1.21922
C14-N13	2.4851072	2.6151162	2.7521585	2.550753	1.60364
N22-C15	1.3425598	1.3648472	1.1523757	1.3990587	1.36976
C24-N23	2.4293309	2.3138288	2.2440847	2.3484169	2.375025
C28-N27	1.4308501	1.4306165	1.5105538	1.4286202	1.358347
N45-C44	1.4369328	1.3743734	1.4635699	1.3976842	1.370042
O46-C44	1.2391514	1.2967463	1.3490889	1.2652729	1.269845
N48-C47	1.2856163	1.3174084	1.3831214	1.3294661	1.265656
C49-N4	1.3505834	1.3713561	1.4370666	1.3705226	1.395935
C50-N48	1.3552004	1.3747616	1.438784	1.3773546	1.305634
N54-C50	1.3661941	1.3809157	1.2268407	1.375835	1.311126

Zr^{+2} complex		Ni^{+2} complex		Ba^{+2} complex		Cu^{+2} complex	
Zr89-O87	1.792592	Ni88-N13	1.78384	Ba88-N23	2.30067	O91-C14	1.385641
Zr89-N54	2.205855	Ni88-O90	1.64846	Ba88-O26	2.3614	Cu92- N48	2.511504
O90-Zr89	1.78707	Ni89-N54	1.82018	Ba89-N48	2.32862	Cu93-N90	2.417429

Table S3

Selected calculated bond angles [°] for ligand and metal complexes

Angle	Ligand	Zr^{+2} complex	Ni^{+2} complex	Ba^{+2} complex	Cu^{+2} complex
N11-C9-C7	36.038634	125.01221	111.01978	35.092056	115.1945
O12-C9-C7	119.95526	94.631367	120.42627	88.715914	116.8096
N13-C10-C9	134.90826	112.76526	105.05712	124.72992	124.6363
C14-N13-C10	152.15495	119.60255	128.73203	141.60652	105.4174
C15-N13-C14	27.845023	140.08967	13.83729	165.78147	109.0268
C17-C15-N13	141.38676	125.47268	98.58692	130.42284	135.0306
H19-C14-N13	94.210793	102.73663	110.27224	97.940828	111.3392
N22-C15-N13	111.56988	104.03602	23.034609	28.942513	109.3465
N23-C16-C15	143.70809	123.67043	108.95162	128.4596	111.30973
C24-N23-C16	166.75269	155.5603	177.49594	150.91703	150.98939
C25-N23-C16	158.98864	142.09255	140.93235	145.79547	149.8149
O26-C24-N23	98.355023	91.64386	78.281407	92.970103	94.6774
N27-C24-N23	132.78311	141.78932	146.41317	140.30583	146.6738
N45-C44-C39	33.803667	28.589213	109.10807	34.37228	92.5908
O46-C44-C39	93.448943	99.237801	110.68447	92.653026	112.2974
C49-N4-C1	179.77163	144.23024	140.6656	142.75181	143.7659
C51-C50-N48	128.23582	134.36774	161.83033	130.35349	131.6464
C52-C49-N4	126.70335	134.629	161.41359	130.50019	151.6861
N54-C50-N48	113.29895	102.74245	85.446002	110.36582	104.5776
C66-C1-N4	124.44843	131.44729	132.21709	128.86044	129.599

Zr^{+2} complex		Ni^{+2} complex		Ba^{+2} complex		Cu^{+2} complex	
O- Zr = O	89.69	N- Ni- O	83.36	N- Ba- N	102.99	N- Cu- O	88.95
O- Zr - O	102.13	O- Ni- N	110.53	O- Ba- N	61.46	O- Cu- O	91.36
O- Zr – N	91.84	N- Ni- N	59.77	N- Ba- O	49.98	O - Cu-N	88.06

Table S4
Calculated molecular orbital energy values of the ligand and metal complexes

Property	Ligand	Zr complex	Ni complex	Ba complex	Cu complex
E_{total} (Hartree)	-2583.5414	-2860.2273	-3107.2850	-2667.4827	-3085.8781
Dipole moment (Debye)	14.2375	16.4800	6.7305	9.3231	8.1660
E_{HOMO} (eV)	-5.2775	-5.0466	-5.2584	-4.8203	-4.5188
E_{LUMO} (eV)	-3.1760	-3.4486	-3.2005	-2.8979	-3.3485
E_{LUMO} - E_{HOMO} (eV)	2.10148	1.5976	2.0579	1.9224	1.1703
***IP* (eV)**	5.2775	5.0466	5.2584	4.8203	4.5188
***EA* (eV)**	3.1760	3.4486	3.2005	2.8979	3.3485
χ (eV)	4.2265	4.2474	4.2294	3.8591	3.9336
μ (eV)	-4.2265	-4.2474	-4.2294	-3.8591	-3.9336
η (eV)	1.0507	0.7988	1.0289	0.9612	0.5851
***S* (eV)**	0.95170	1.2518	0.9719	1.0403	1.7091

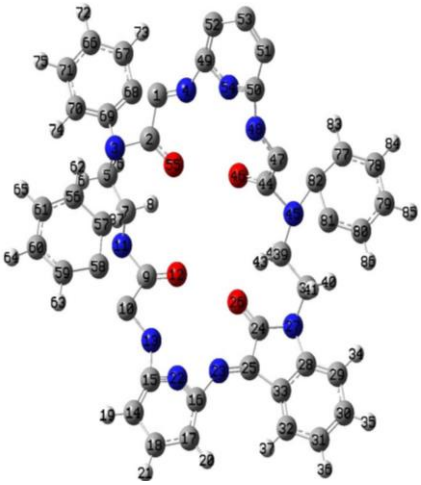

Fig. S3. The optimized structures of ligand with atoms numbers

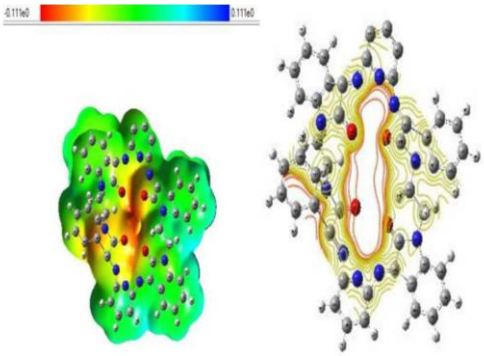

Fig. S4. MEP of the Ligand

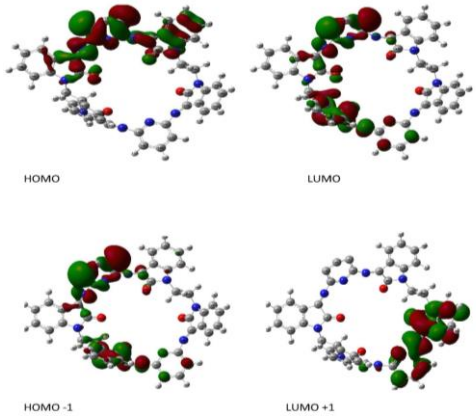

Fig. S5. The HOMO and LUMO frontier molecular orbitals of the ligand.